Project Number: MQP-REC-0032

Synthesis and Photophysical Properties of an Asymmetrically Substituted 2,5-Diarylidene Cyclopentanone Dye: (2E, 5E)-2-(benzofuran-2-ylmethylene)-5-(4-(dimethylamino)benzylidene)cyclopentanone

A Major Qualifying Project Report

Submitted to the Faculty of

WORCESTER POLYTECHNIC INSTITUTE

In partial fulfillment of the requirements for the

Degree of Bachelor of Science

By:

Meghan A. Roache

April 29, 2010

Approved by:

Prof. Robert E. Connors, Ph.D.
Project Advisor

Abstract

This work extends our interest in the spectroscopic and photophysical properties of symmetrically substituted 2,5-diarylidene cyclopentanones to asymmetrically substituted 2,5-diarylidene cyclopentanone dyes. Attention is given to (2E,5E)-2-(benzofuran-2-ylmethylene)-5-(4-(dimethylamino)benzylidene)cyclopentanone (**bydbc**). Compound **bydbc** was synthesized via a two-step reaction; the first step involved a DIMCARB-catalyzed reaction of cyclopentanone with 2-benzofurancarboxaldehyde to form the benzofuran monoarylidene cycloadduct, (E)-2-(benzofuran-2-ylmethylene)cyclopentanone (**asbf**), while the second step involved the base-catalyzed reaction of **asbf** with p-dimethylaminobenzaldehyde to form **bydbc**. Spectroscopic and photophysical properties of **bydbc** have been measured in a wide variety of nonpolar and polar protic and aprotic solvents. Fluorescence quantum yields and fluorescence lifetimes show a strong solvent dependence. The fluorescence quantum yields ranged from $4.92*10^{-3}$ (n-hexane) to 0.135 (CH_2Cl_2) and fluorescence lifetimes ranged from 0.16 ns (acetone) to 1.1 ns (CH_2Cl_2). First-order radiative and nonradiative decay constants have been calculated from the fluorescence quantum yield and lifetime data. The photophysical properties and spectral data show a correlation with the $E_T(30)$ empirical solvent polarity scale. B3LYP/6-31G(d) geometry optimization and TD-DFT spectral calculations were performed on **bydbc**.

Acknowledgements

I would like to thank Professor Robert E. Connors for the use of his laboratory as well as all of the help and guidance he gave me through the course of this project. I would also like to thank Christopher Zoto for all of his assistance, guidance, patience, and time.

Table of Contents

Introduction

A conjugated compound is one which contains carbon-carbon double bonds in a 1,3-conformation; the conjugation depends on the overlap of p atomic orbitals. One such class of organic conjugated compounds is 2,5-diarylidene cyclopentanone dyes. These have been shown to have a number of applications. For instance, these compounds have been used as photosensitizers[1], fluorescent solvent polarity probes[2,3], fluoroionophores[4], and nonlinear optical materials[5]. The general structure of these dyes is shown below in Figure 1.

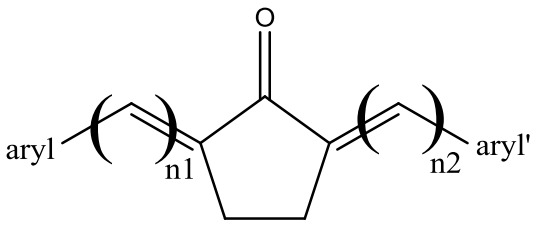

Figure 1: General structure of 2,5-diarylidene cyclopentanone dyes.

Much research has been done in compounds where aryl=aryl' and n1=n2[6,7]. This report will extend to a compound where aryl≠aryl' and n1≠n2, or in other words to an asymmetrically substituted 2,5-diarylidene cyclopentanone dye. The structure of (2E,5E)-2-(benzofuran-2-ylmethylene)-5-(4-(dimethylamino)benzylidene)cyclopentanone (**bydbc**), is shown in Figure 2. The electronic structure and spectroscopy of **bydbc** were studied in a variety of nonpolar as well as polar aprotic and protic solvents, and investigation of these characteristics provides insight into the photophysical and solvatochromic properties of this compound.

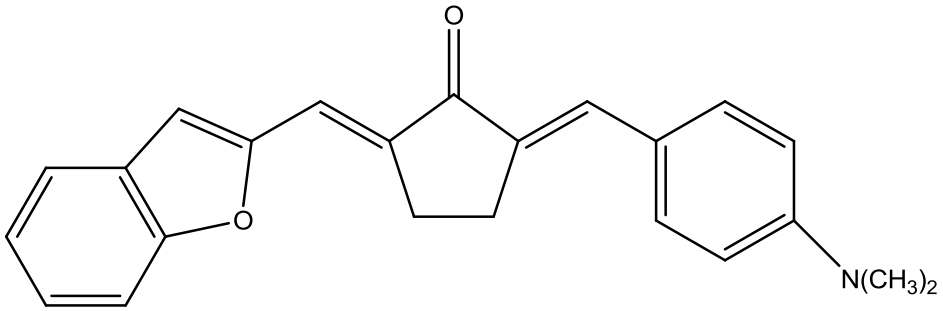

Figure 2: (2E,5E)-2-(benzofuran-2-ylmethylene)-5-(4-(dimethylamino)benzylidene)cyclopentanone (**bydbc**).

Solvatochromism is the influence of a solvent on the electronic absorption and emission spectra of molecules, or the ability of a substance to change color with respect to the polarity of its solvent[8]. Depending on the solvent, solvatochromic molecules can undergo one of two transitions: hypsochromic (blue) shifts or bathochromic (red) shifts. Previous solvatochromic studies of analogous dyes have shown a bathochromic shift when going from nonpolar to polar protic solvents.

Finally, quantum mechanical calculations were performed on **bydbc** using B3LYP/6-31G(d) geometry optimization and TD-DFT spectral calculations. These calculations show that the $S_0 \rightarrow S_1$ transition occurs via an intramolecular charge transfer (ICT) (π, π^*) mechanism, and that the $S_0 \rightarrow S_2$ transition is predicted to be (n, π^*).

Experimental

Synthesis of bydbc

As illustrated in Figure 3, compound **bydbc** was synthesized via a two-step reaction. The first step involved reacting cyclopentanone (5.0 mmol, 0.44 mL) with 2-benzofurancarboxaldehyde (5.0 mmol, 0.61 mL) in the presence of DIMCARB (27.5 mmol, 3.3 mL) in dichloromethane (5.5 mL) with continuous stirring at room temperature. DIMCARB, or N,N-dimethylammonium-N',N'-dimethylcarbamate, has been shown by others to give moderate to excellent yields of monoarylidene ketone adducts[9,10]. Although DIMCARB reactions can be portrayed as mono-Claisen-Schmidt reactions, the mechanism occurs via a Mannich-type pathway. The reaction was monitored by TLC, confirming reaction completion at approximately 2 hours. The solvent was removed *in vacuo*, leaving behind an oily substance. The crude material was acidified with 0.5 M H_2SO_4 (10 mL). The organic layer was then collected by extracting with dichloromethane (3 x 25 mL) and dried overnight over anhydrous sodium sulfate (Na_2SO_4). Purification consisted of running silica gel column chromatography, employing a gradient approach of hexanes and ethyl acetate, which afforded the pure (E)-2-(benzofuran-2-ylmethylene)cyclopentanone (**asbf**) as a yellow solid. Purity was confirmed by TLC, showing one spot upon development. ^{1}H and ^{13}C NMR spectroscopy were used to confirm the structure of **asbf** (see Figure 4).

The second step consisted of running a crossed-aldol condensation reaction of **asbf** (1.65 mmol, 0.35 g) with p-dimethylaminobenzaldehyde (1.65 mmol, 0.25 g) in the presence of 2.5% (w/v) NaOH (1 mL). Ethanol (150 mL) was used as the solvent for this reaction. The red-colored reaction solution was allowed to run overnight with continuous stirring at room temperature. A precipitate was collected via vacuum filtration, washed with cold ethanol, dried, and purified by

silica gel column chromatography. ^{1}H and ^{13}C NMR confirmed the structural identity of **bydbc** (see Figure 5) and purity was confirmed by TLC (one spot upon development).

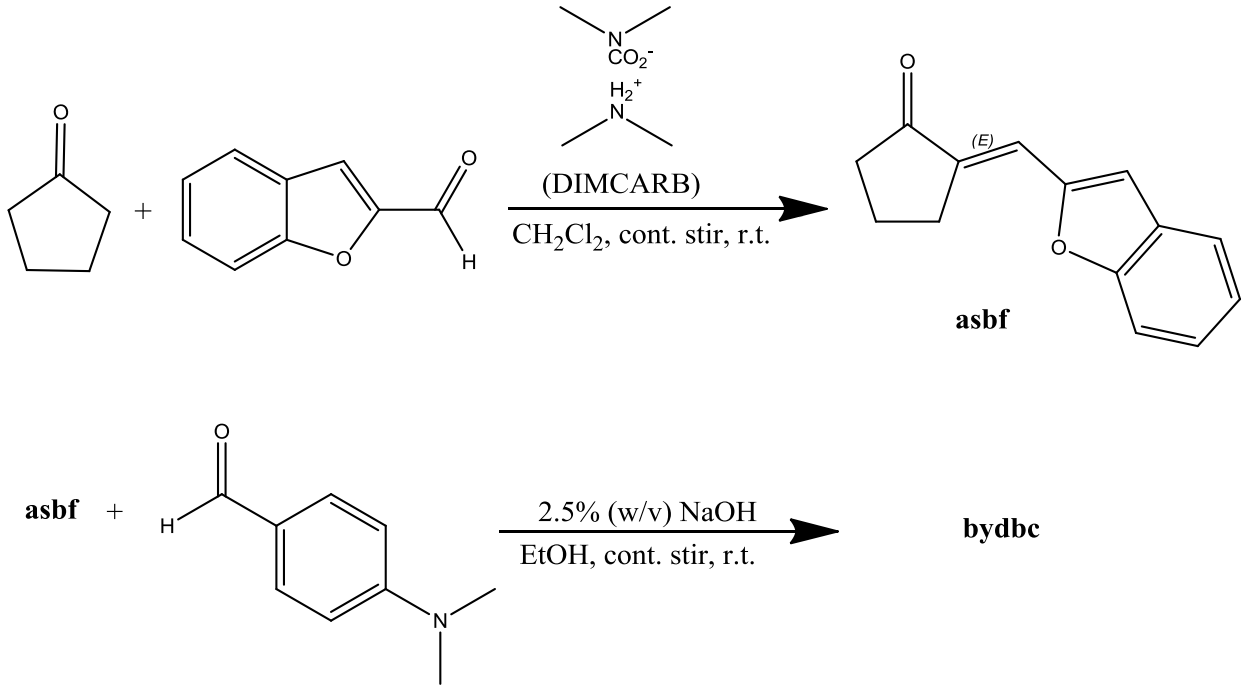

Figure 3: Reaction scheme for the synthesis of **bydbc**.

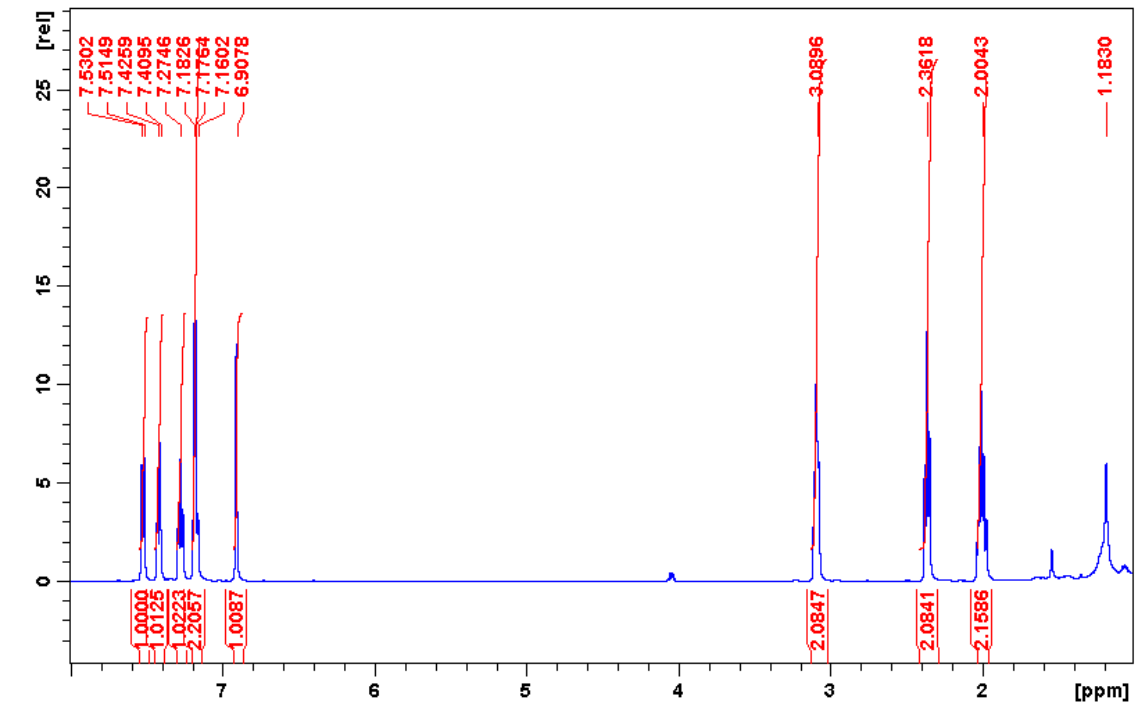
[rel]
25
20
15
10
5
0
7.5302
7.5149
7.4259
7.4095
7.2746
7.1826
7.1764
7.1602
6.9078
3.0896
2.3618
2.0043
1.1830
1.0000
1.0125
1.0223
2.2057
1.0087
2.0847
2.0841
2.1586
7
6
5
4
3
2
[ppm]

(a)

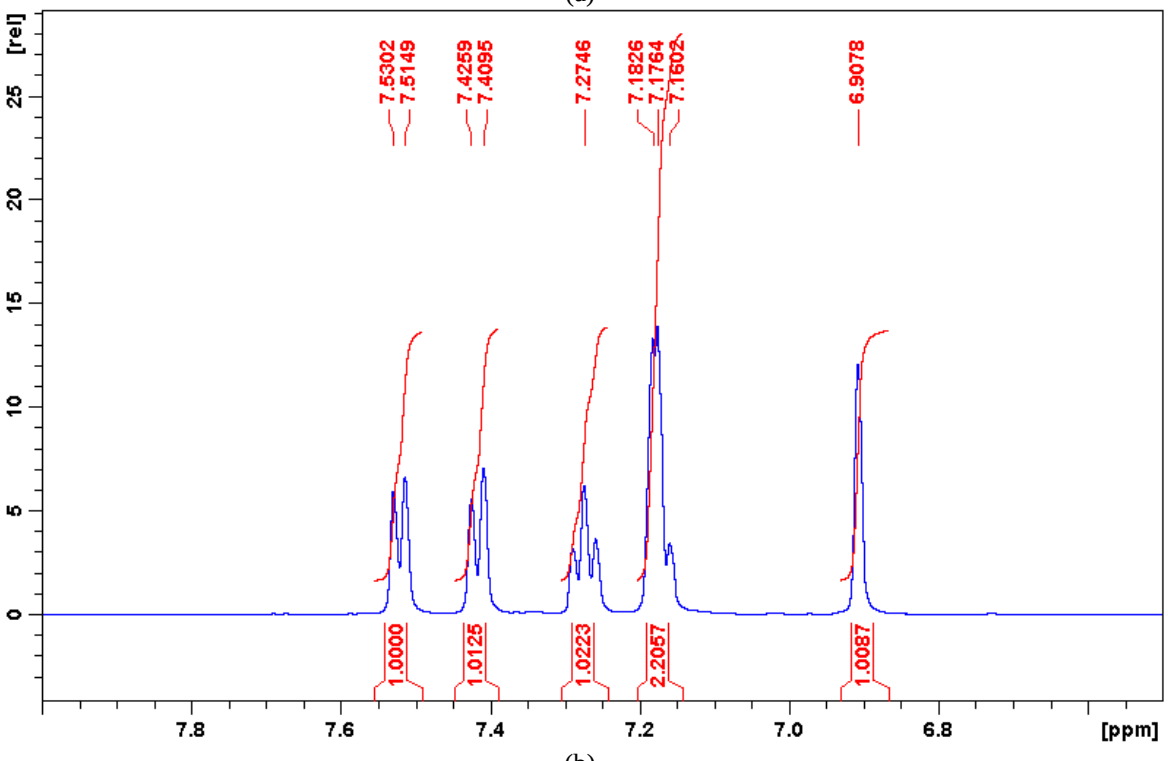
[rel]
25
20
15
10
5
0
7.5302
7.5149
7.4259
7.4095
7.2746
7.1826
7.1764
7.1602
6.9078
1.0000
1.0125
1.0223
2.2057
1.0087
7.8
7.6
7.4
7.2
7.0
6.8
[ppm]

(b)

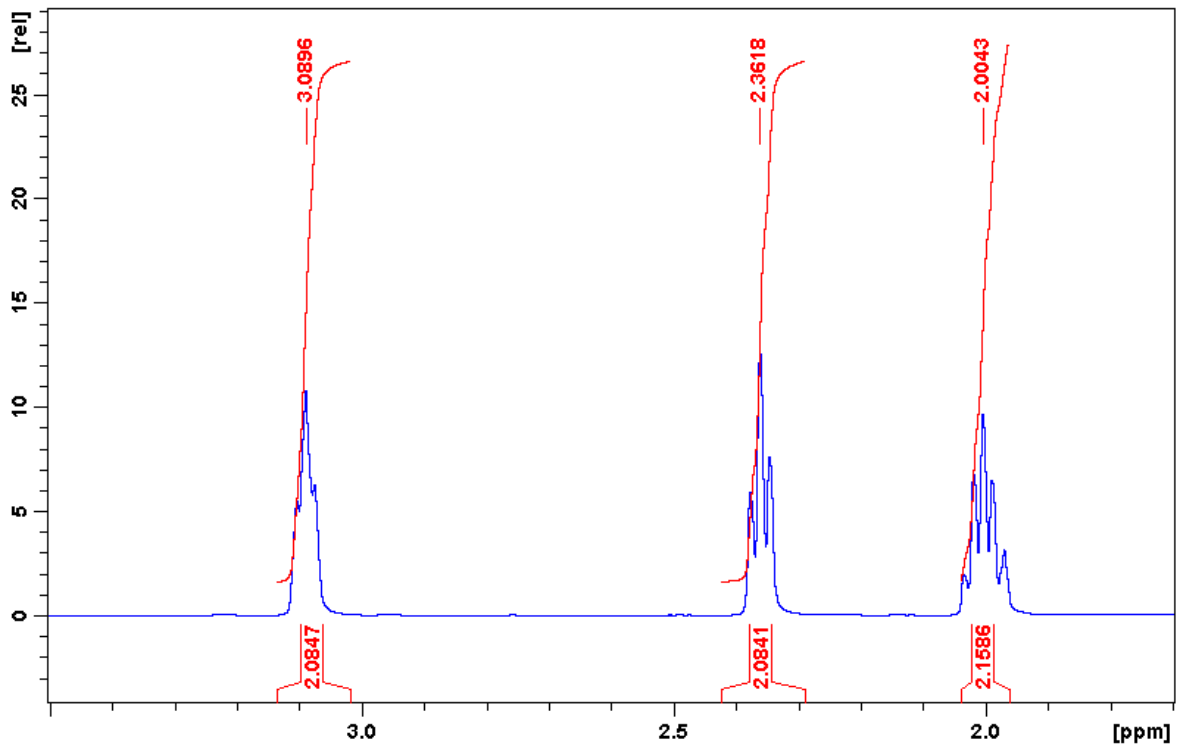

(c)

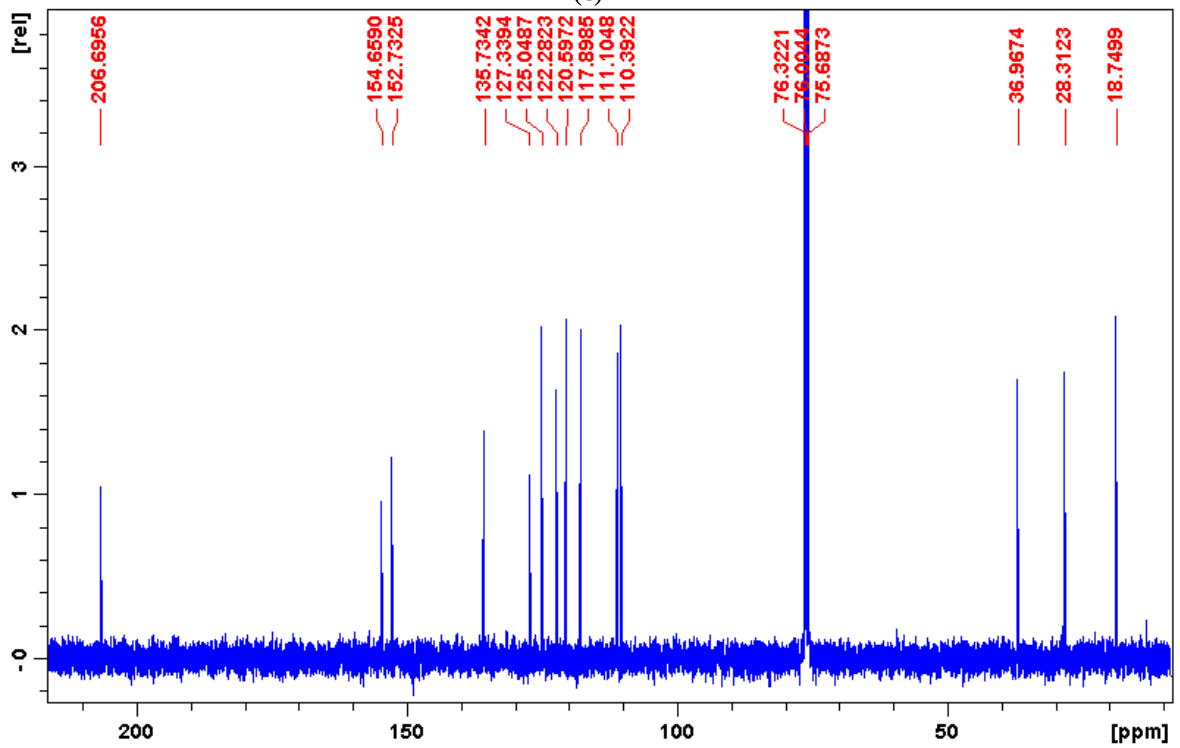

(d)

Figure 4: (a) ^{1}H δ 1-8 ppm, (b) ^{1}H δ 6.5-8 ppm, (c) ^{1}H δ 1.7-3.5 ppm and (d) ^{13}C NMR spectra of **asbf** in $CDCl_3$. ^{1}H NMR: δ (ppm) = 7.52 (1H), 7.41 (1H), 7.27 (1H), 7.18-7.16 (2H), 6.91 (1H), 3.09 (2H), 2.36 (2H), 2.00 (2H). ^{13}C NMR: δ (ppm) = 206.70, 154.66, 152.73, 135.73, 127.34, 125.05, 122.28, 120.60, 117.90, 111.10, 110.39, 36.97, 288.31, 18.75.

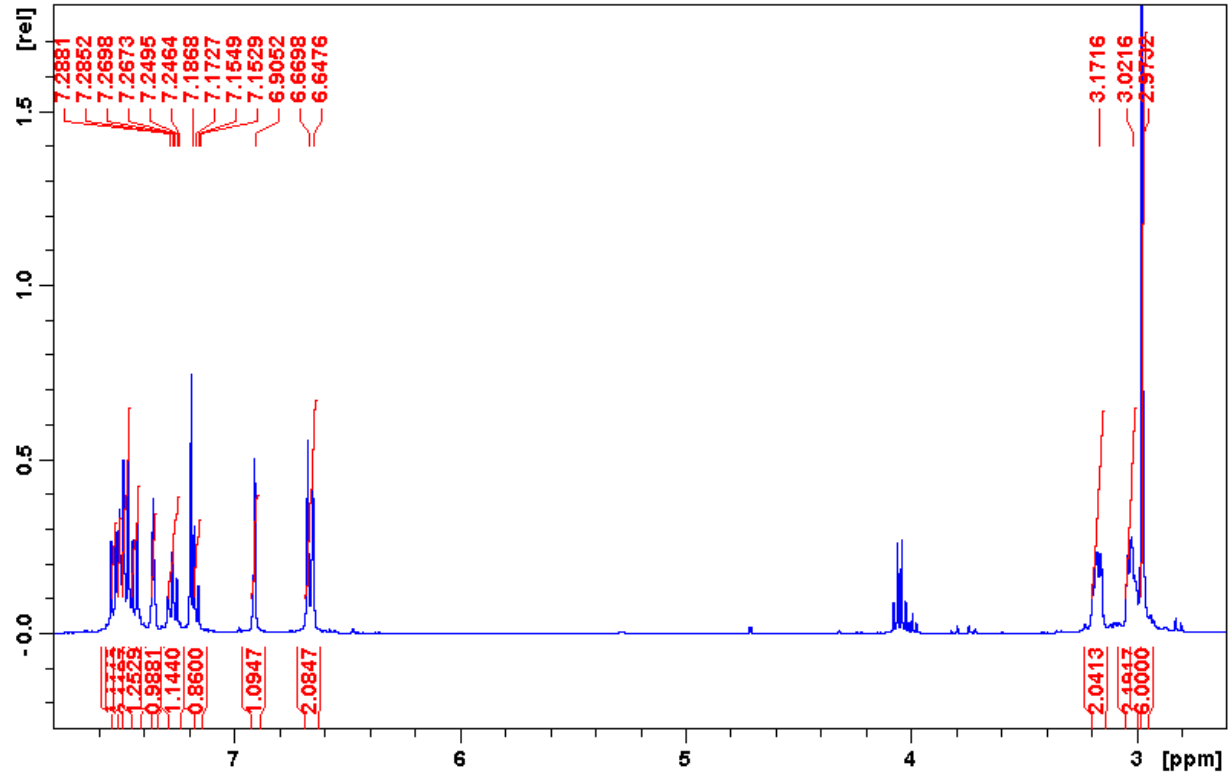
[rel]
1.5
1.0
0.5
-0.0
7.2881
7.2852
7.2698
7.2673
7.2495
7.2464
7.1868
7.1727
7.1549
7.1529
6.9052
6.6698
6.6476
3.1716
3.0216
2.9732
1.2529
0.9881
1.1440
0.8600
1.0947
2.0847
2.0413
2.1917
6.0000
7
6
5
4
3
[ppm]

(a)

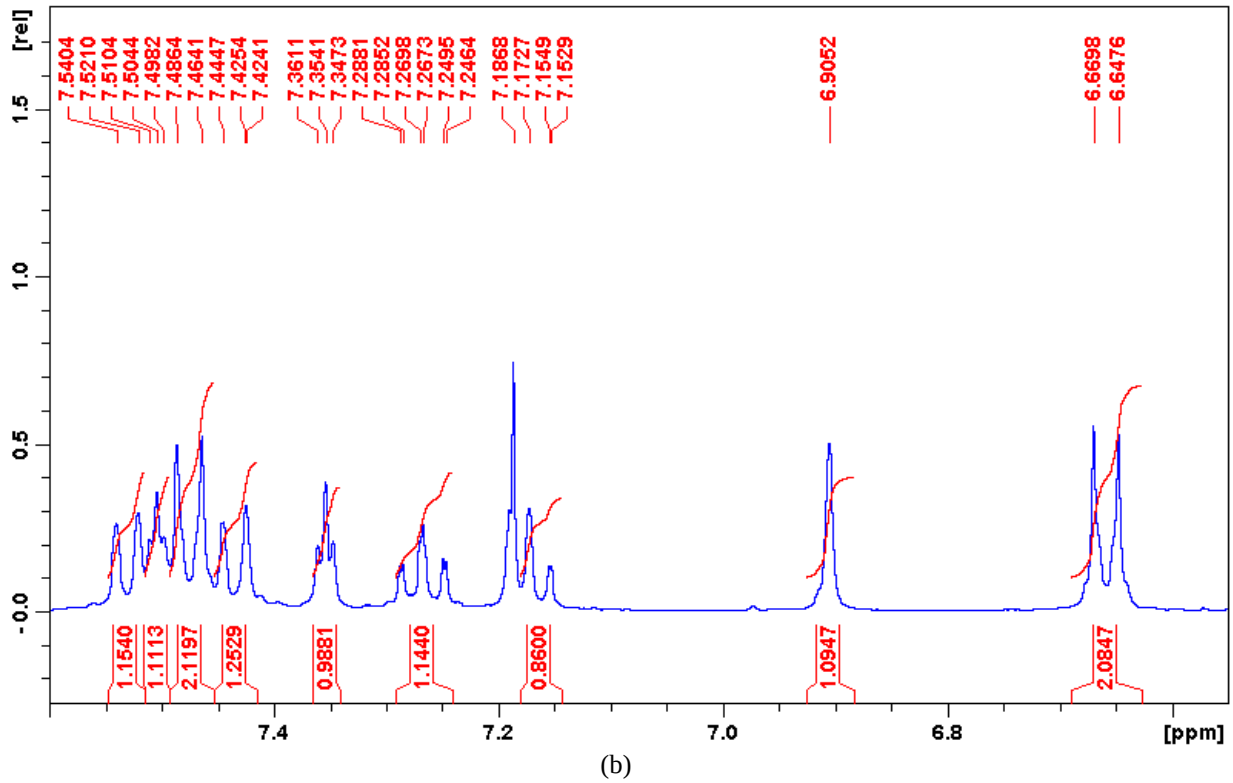
[rel]
1.5
1.0
0.5
-0.0
7.5404
7.5210
7.5104
7.5044
7.4982
7.4864
7.4641
7.4447
7.4254
7.4241
7.3611
7.3541
7.3473
7.2881
7.2852
7.2698
7.2673
7.2495
7.2464
7.1868
7.1727
7.1549
7.1529
6.9052
6.6698
6.6476
1.1540
1.1113
2.1197
1.2529
0.9881
1.1440
0.8600
1.0947
2.0847
7.4
7.2
7.0
6.8
[ppm]

(b)

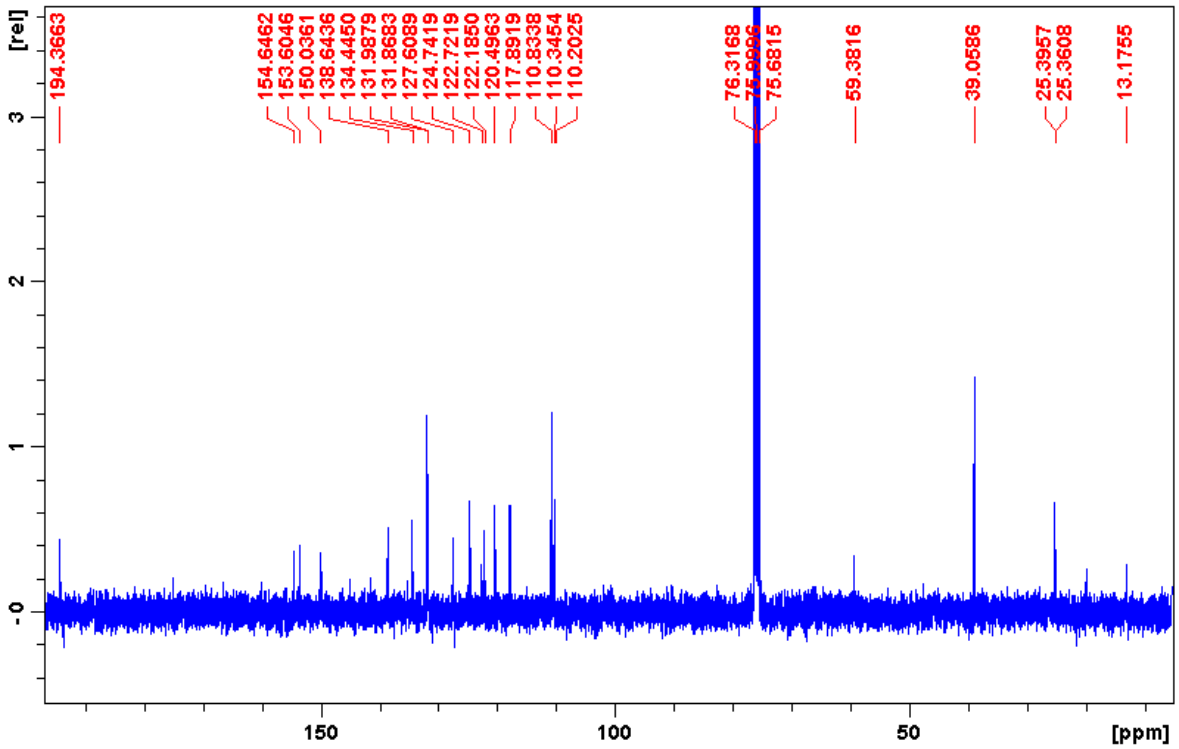

(c)

Figure 5: (a) ^{1}H δ 7.8-2.6, (b)^{1}H δ 7.6-6.6, and (c) ^{13}C NMR spectra of **bydbc** in $CDCl_3$. ^{1}H NMR: δ (ppm) = 7.54-7.42 (5H), 7.35 (1H), 7.27 (1H), 7.15 (1H), 6.91 (1H), 6.66 (2H), 3.17 (2H), 3.02 (2H), 2.97 (6H). ^{13}C NMR: δ (ppm) = 194.36, 154.64, 153.60, 150.03, 138.64, 134.44, 131.98, 131.86, 127.61, 124.74, 122.72, 122.18, 120.49, 117.89, 110.83, 110.34, 110.20, 39.06.

Spectrophotometric Analysis

UV/Vis absorption spectra were collected on a Shimadzu UV 2100U spectrometer with 2-nm band-pass. The fluorescence spectra were collected on a Perkin-Elmer® LS 50B luminescence spectrophotometer with an R928 phototube detector. The NMR spectra were measured with a Bruker® AVANCE 400 MHz spectrometer.

Determination of Fluorescence Quantum Yields

The fluorescence yield of a compound, Φ_f, is defined as the ratio of photons emitted to the number of photons which were originally absorbed by the compound, and is calculated by the equation[11]

$$\Phi_c = \Phi_s \frac{A_s}{A_c} \frac{{n_c}^2}{{n_s}^2} \frac{D_c}{D_s} \qquad (eq.\ 1)$$

where the fluorescence quantum yield of the standard, Φ_s, is obtained from the literature, A is the absorbance value at a fixed wavelength of excitation, n is the refractive index of the solvents used, and D is the calculated area under the corrected emission spectrum; the subscript s refers to the standard, while the subscript c refers to the compound being studied.

Fluorescence quantum yields of **bydbc** were calculated by preparing a stock solution with a maximum absorbance of approximately 0.5. The stock solution was accurately diluted tenfold and optical absorption spectra of both the stock solution and the diluted solution were collected. A fluorescence emission spectrum of the tenfold diluted solution was recorded, fixing the excitation wavelength at λ=450 nm. Absorption and fluorescence emission spectra were obtained for the standard, fluorescein in 0.1 N NaOH (Φ_f = 0.95). Microsoft Excel® was used to convert the spectral data from wavelength to wavenumbers. The analysis was completed by Mathcad®, which corrected the emission spectra of the standard and the compound being studied. In order to correct the fluorescence emission spectra for instrument response, the literature emission

spectrum of N,N-dimethylamino-3-nitrobenzene (N,N-DMANB)[12] was compared to the experimental emission spectrum of N,N-DMANB measured using the LS-50B spectrometer. A set of scale factors were determined every 50 cm^{-1} between 12,500 cm^{-1} and 22,200 cm^{-1}. A sample calculation of the fluorescence quantum yield of **bydbc** can be found in Appendix A.

Determination of Fluorescence Lifetimes

The fluorescence lifetime of a compound, τ_f, is equal to the inverse of the sum of the first-order radiative and non-radiative rates of decay:

$$\tau_f = \frac{1}{k_f + k_{nr}} \qquad (eq.\ 2)$$

The fluorescence lifetimes of **bydbc** were measured using a Photon Technology International® fluorescence lifetime spectrometer equipped with a GL-3300 nitrogen laser and GL-302 dye laser. In order to prevent quenching by molecular oxygen of the excited state, each solution was degassed with molecular nitrogen for at least five minutes prior to measuring the fluorescence decay curves. FeliX32 was the software used to measure the fluorescence decay curves. The fluorescence decay profile of the instrument response function (IRF) was generated at the same maximum intensity as the decay curve of the compound being studied; an aqueous non-dairy creamer solution in DI water was used to scatter the excitation beam. Neutral density filters were used appropriately to adjust the fluorescence intensity of the IRF profile. Upon generating the time-dependent fluorescence decay spectra as well as the IRF, the lifetimes were measured via a curve-fitting procedure; the best-fit curves were chosen based on how well the field-fit curve aligned to the sample curve based on statistical analysis. A sample calculation for fluorescence lifetime determination of **bydbc** can be found in Appendix B.

Results and Discussion

The electronic absorption and fluorescence properties of **bydbc** were measured in twelve solvents. As a means of illustrating the solvatochromic nature of this compound, the absorption and fluorescence emission spectra of **bydbc** in six nonpolar and polar aprotic and protic solvents are presented in Figure 6. Experimental data shows that **bydbc** undergoes a bathochromic shift in going from nonpolar to polar solvents. When dissolved in nonpolar solvents, **bydbc** was yellow in color; when dissolved in polar protic solvents, **bydbc** was light orange in color. Additionally, as the polarity increases, so does the broadening of the spectra. It can also be seen from Figure 6 that the fluorescence spectra undergo a greater bathochromic shift than do the absorption spectra.

The photophysical characteristics of **bydbc** in twelve solvents are shown in Table 1. Also listed are both the solvent polarity function (Δf) and the empirical scale of solvent polarity ($E_T(30)$) of each solvent. The solvent polarity function (Δf) is dependent upon the dielectric constant (E) and the index of refraction (n) of the solvent, mathematically defined as

$$\Delta f = \frac{E-1}{2E+1} - \frac{n^2-1}{2n^2+1} \qquad (eq.\ 3)$$

The $E_T(30)$ empirical solvent polarity scale is based on the solvatochromic shift of the first maximum of a betaine dye[8].

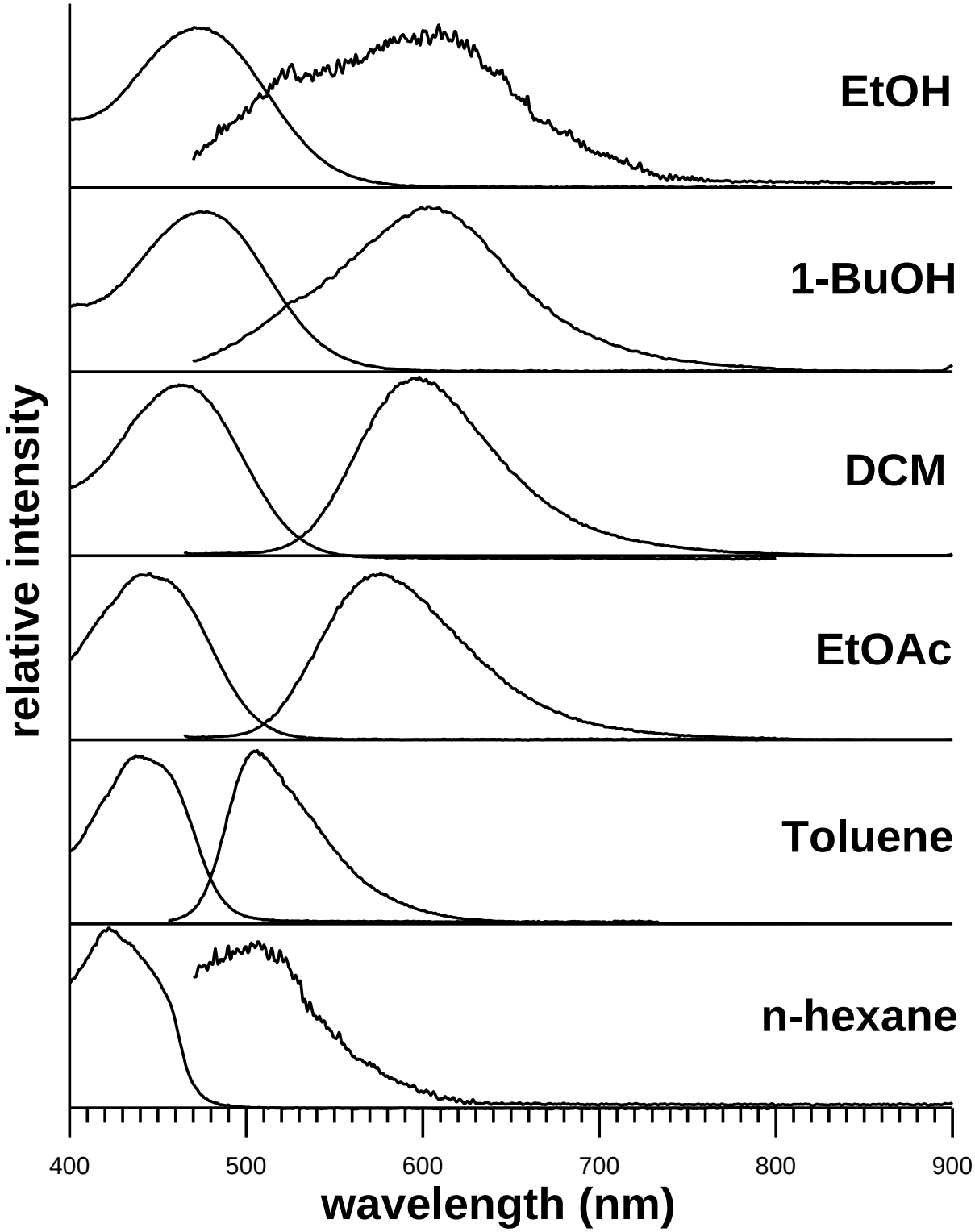

Figure 6: Electronic absorption and fluorescence spectra of **bydbc** in solvents of various polarities.

Table 1: Spectroscopic and photophysical characteristics of **bydbc** in various solvents.

Solvent	ν_{abs} (cm^{-1})	ν_{fl} (cm^{-1})	Δf*	$E_T(30)$* (kcal mol^{-1})	Φ_f	τ_f (ns)	k_f (s^{-1})	k_{nr} (s^{-1})
EtOH	21254 (471 nm)	15510 (645 nm)	0.2887	51.9	9.70E-03	0.23	4.22E+07	4.31E+09
1-PrOH	21164 (473 nm)	15690 (637 nm)	0.2746	50.7	0.016	0.30	5.33E+07	3.28E+09
1-BuOH	21075 (475 nm)	15760 (635 nm)	0.2642	50.2	0.046	0.26	1.77E+08	3.67E+09
DMSO	21053 (475 nm)	13470 (742 nm)	0.2637	45.1	0.017	0.23	7.39E+07	4.27E+09
Acetone	21954 (456 nm)	15460 (647 nm)	0.2843	42.2	0.034	0.16	2.13E+08	6.04E+09
CH_2Cl_2	21645 (462 nm)	16250 (615 nm)	0.2171	40.7	0.135	1.1	1.23E+08	7.86E+08
EtOAc	22447 (446 nm)	16785 (596 nm)	0.1996	38.1	0.088	0.64	1.38E+08	1.43E+09
EtBz	21529 (465 nm)	16680 (600 nm)	0.1581	38.1	0.133	0.81	1.64E+08	1.07E+09
Toluene	22472 (445 nm)	18810 (532 nm)	0.0131	33.9	0.049	0.31	1.58E+09	3.07E+09
CS_2	21739 (460 nm)	19050 (525 nm)	-0.0007	32.8	0.040	0.19	2.11E+08	5.05E+09
CCl_4	22701 (441 nm)	19920 (502 nm)	0.0119	32.4	0.021	0.30	7.00E+07	3.26E+09
n-hexane	23697 (422 nm)	19275 (519 nm)	-0.0004	31	4.92E-03	--	--	--

*[2] Both Δf and $E_T(30)$ values are taken from Suppan, P. and Ghonheim, N., in *Solvatochromism*, The Royal Society of Chemistry, Cambridge, 1997.

Absorption and fluorescence properties of **bydbc** were plotted against both Δf and $E_T(30)$ (see Figures 7 and 8). These plots illustrate the solvatochromic properties of **bydbc**, with solvatochromism being more pronounced in the fluorescence spectral data. The compound shifts from 502 nm (in CCl_4) to 742 nm (in DMSO). The observed solvatochromic properties are consistent with a charge transfer electronic transition.

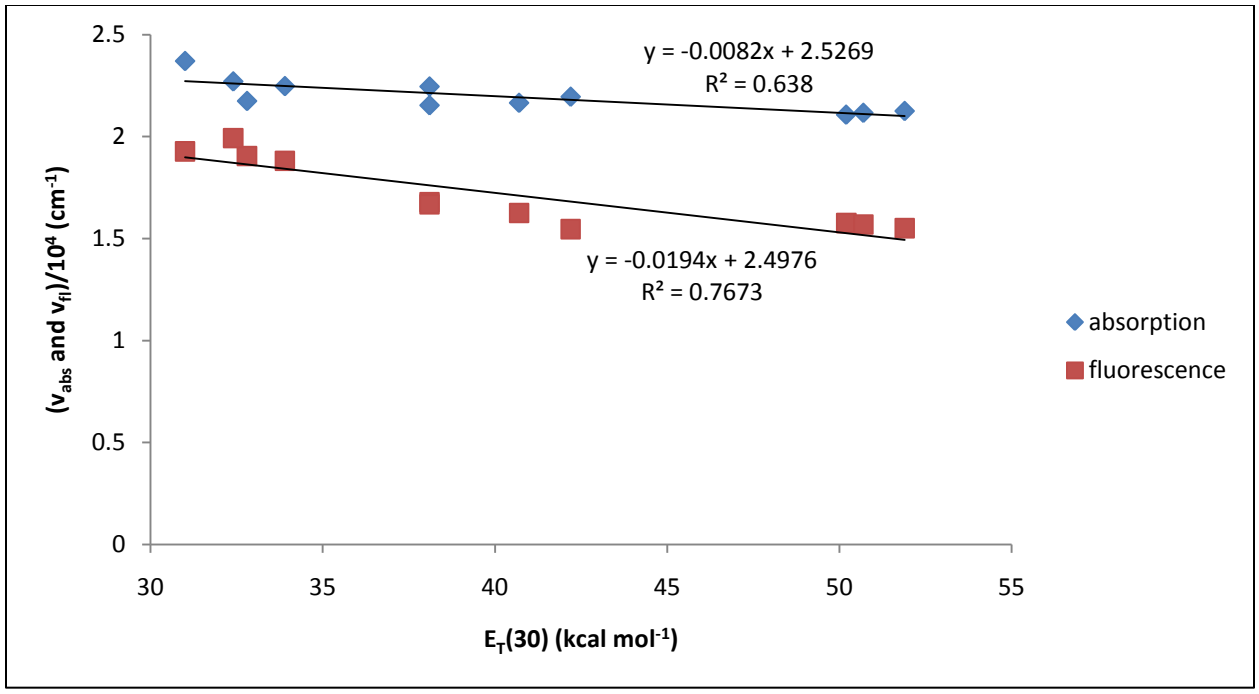

Figure 7: Plot of maximum absorption and fluorescent wavenumbers of **bydbc** against Δf in various solvents.

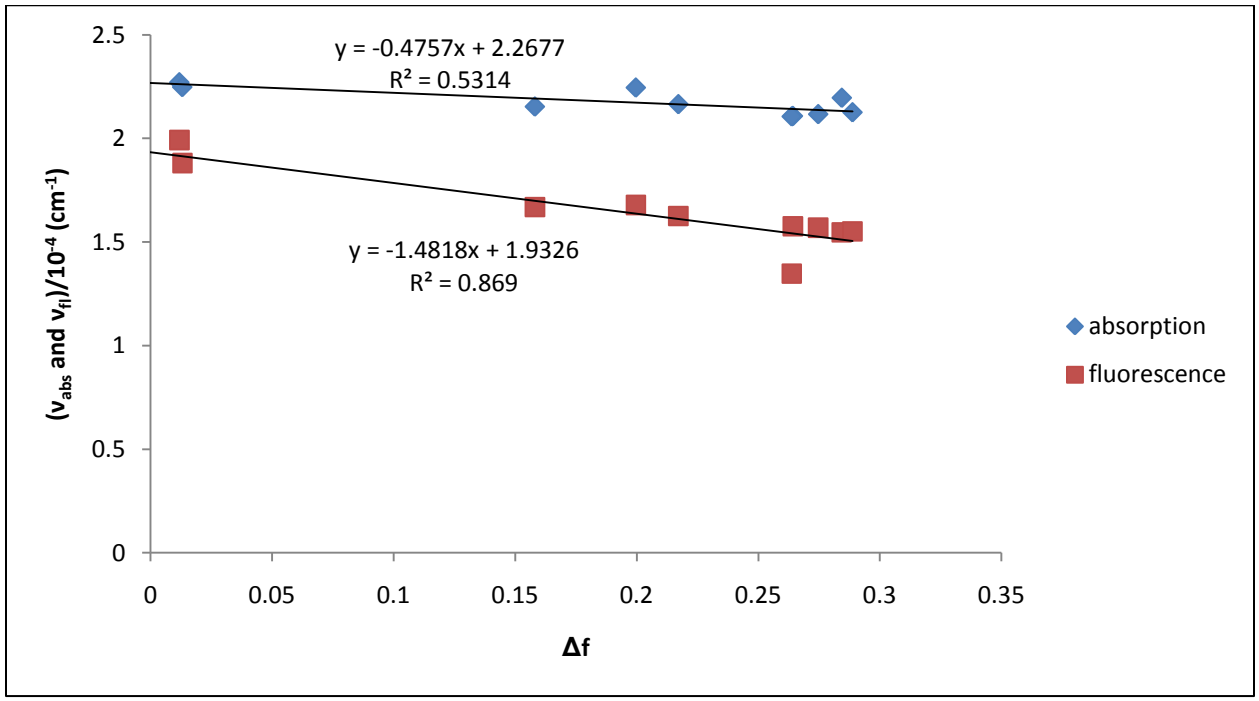

Figure 8: Plot of maximum absorption and fluorescent wavenumbers of **bydbc** against $E_T(30)$ in various solvents.

Data collected experimentally from the fluorescence quantum yields, Φ_f, as well as the fluorescence lifetimes, τ_f, show a strong solvent dependence for the compound. These values

were used to calculate the first-order radiative and nonradiative decay constants for the first excited singlet state of **bydbc**. The first-order radiative decay constant, k_f, is given by:

$$k_f = \frac{\Phi_f}{\tau_f} \qquad (eq.\ 4)$$

where Φ_f is the fluorescence quantum yield and τ_f is the fluorescence lifetime. Using that value, the first-order nonradiative decay constant, k_{nr}, can be determined by using the equation:

$$k_{nr} = \left(\frac{1}{\Phi_f} - 1\right) k_f \qquad (eq.\ 5)$$

The fluorescence quantum yields of **bydbc** were also plotted against the maximum fluorescence wavenumbers, ν_{fl}, as shown in Figure 9.

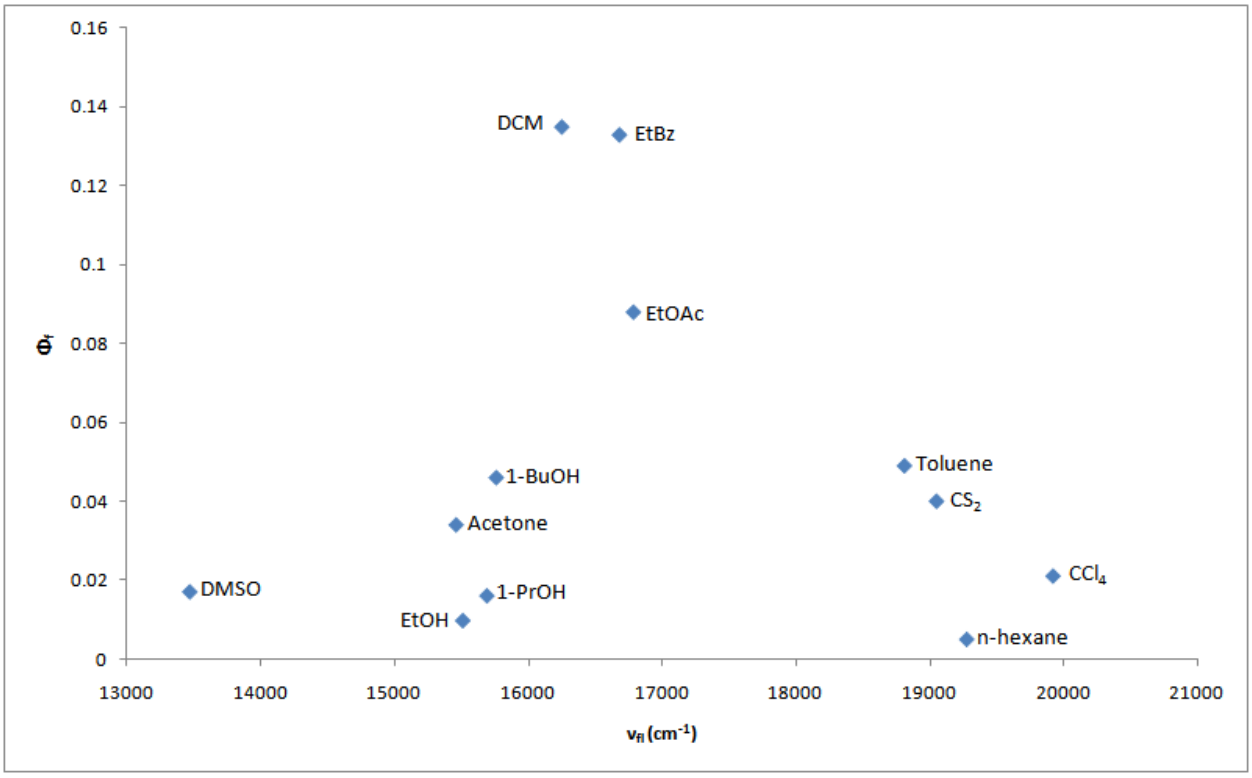

Figure 9: Plot of the fluorescence quantum yields against the maximum fluorescence wavenumbers.

The fluorescence quantum yield of a molecule can be expressed by the equation

$$\Phi_f = \frac{k_f}{k_f + k_{nr}} \qquad (eq.\ 6)$$

where $k_{nr}=k_{ic}+k_{isc}$, k_{ic} is the rate of internal conversion, and k_{isc} is the rate of intersystem crossing.

As discussed later in this section, quantum chemical calculations show that S_1 is (ICT, π, π^*) and S_2 is predicted to be (n, π^*) for **bydbc**. A similar order is predicted for the corresponding triplet states. There is a rule in photoexcited-state systems, called El-Sayed's rule for intersystem crossing, which states that the rate of intersystem crossing between two states of different orbital configurations is larger than that between two states of the same orbital configuration[13]. In nonpolar solvents, Φ_f is low. As solvent polarity gradually increases, the T_2 (n, π^*) state rises higher in energy, which results in a decrease in k_{isc} and thus an increase in Φ_f. Internal conversion and intersystem crossing are competitive processes. As solvent polarity further increases, there comes a point where the increasing rate of internal conversion dominates over the competitive decreasing rate of intersystem crossing, thereby resulting in an overall decrease in Φ_f.

The k_{nr} values of **bydbc** were calculated from equation 5, ranging from $7.86*10^8$ s^{-1} (dichloromethane) to $6.04*10^9$ s^{-1} (acetone). These values were plotted against the corrected maximum fluorescent wavenumbers, as depicted in Figure 10. Specifically, an increase in k_{nr} was observed from 16250 cm^{-1} (CH_2Cl_2) to 15460 cm^{-1} (acetone). The substantial increase in k_{nr} in this region is attributed to the energy gap law for internal conversion which predicts an exponential dependence of the rate of internal conversion (k_{ic}) on ΔE, the S_0-S_1 energy gap[14]

$$k_{ic}=Ce^{-\alpha\Delta E}, \qquad (eq.\ 7)$$

where C and α are constants. According to the energy gap law of internal conversion for photoexcited states, k_{nr} is expected to increase as the S_0-S_1 energy gap decreases due to greater vibrational overlap (Frank-Condon factor) between the S_0 and S_1 states. Also in accordance to

the plot in Figure 10, the k_{nr} decreases mainly from 19920 cm^{-1} (CCl_4) to 16250 cm^{-1} (dichloromethane); this demonstrates anti-energy gap behavior in this region. The deviation from the energy gap law in less polar solvents may be related to the location of the T_2 (n, π^*) state and its influence on intersystem crossing.

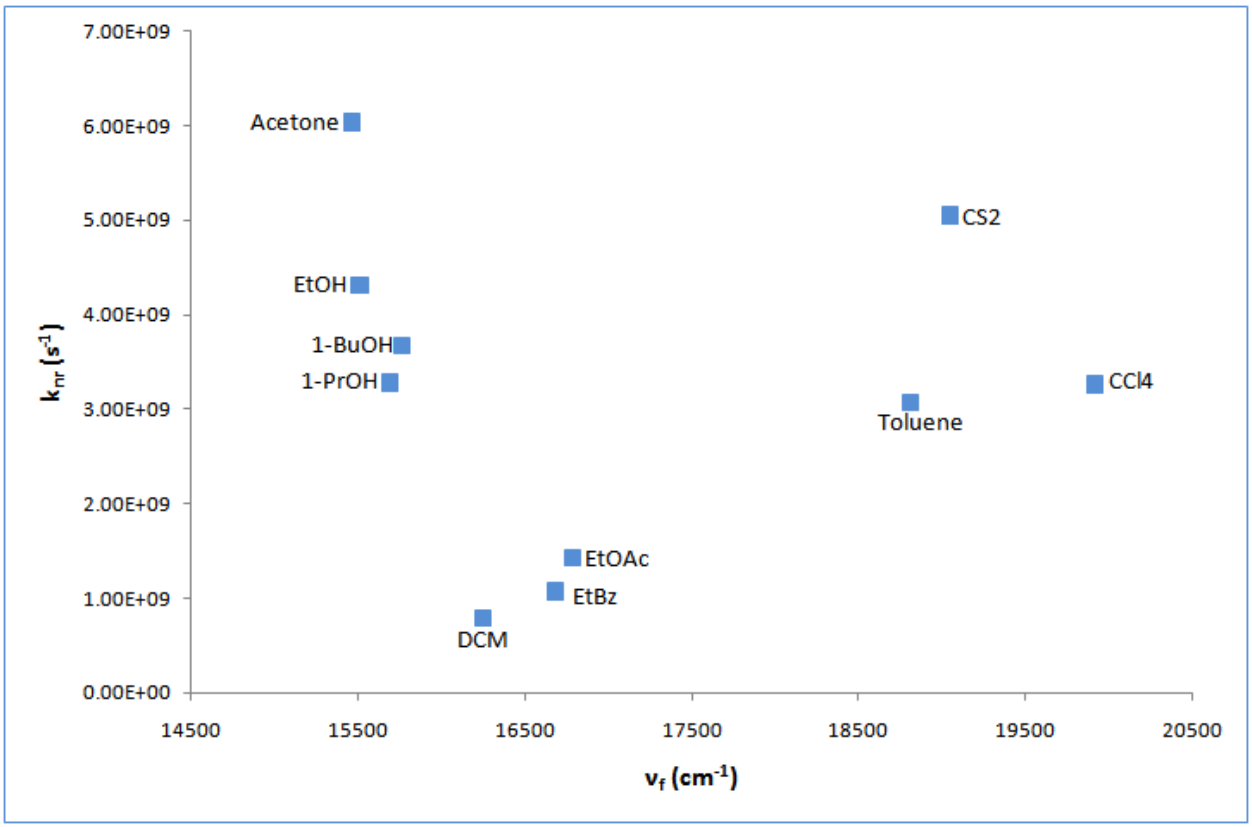

Figure 10: Plot of the first-order nonradiative decay constant (k_{nr}) of **bydbc** against the corrected fluorescent wavenumbers in various solvents.

The excited-state dipole moment of **bydbc** was calculated via the Lippert-Mataga method[15,16]. Shown in Figure 11, a Lippert-Mataga plot directly relates the Stoke's shift (Δν) of **bydbc** against Δf in various solvents. The Stoke's shift (Δν) is defined as the change in wavenumbers between the absorbance and fluorescence spectral maxima. The relationship between Δν and Δf is given by

$$\Delta\upsilon = \Delta\upsilon_0 + \frac{2\Delta\mu^2}{hca^3}\Delta f \qquad (eq.\ 8)$$

where $\Delta\nu_0$ is the Stoke's shift when $\Delta f=0$ (shown on the graph as the y-intercept), h is Planck's constant ($6.626\text{x}10^{-34}$ J•s), c is the speed of light in a vacuum ($2.998\text{x}10^{8}$ m•s^{-1}), a is the Onsager cavity radius for the spherical interaction of the dipole in a solvent, and $\Delta\mu$ is the difference between the excited-state and ground-state electronic dipole moments ($\Delta\mu=\mu_{excited}-\mu_{ground}$). A plot of $\Delta\nu$ against Δf therefore yields a straight line which has a slope of $2\Delta\mu^2/hca^3$; this equation can subsequently be used to calculate the excited-state dipole moment of **bydbc**, since a and μ_{ground} are determined using TD-DFT spectral calculations. These calculations yielded an Onsager cavity radius of 5.45Å and a μ_{ground} of 5.72 D. By using the Lippert-Mataga method, the excited-state dipole moment of **bydbc** was calculated to be 18.6 D. The threefold increase in the electronic dipole moment in going from the ground state to the excited state is attributed to the charge transfer nature of this compound.

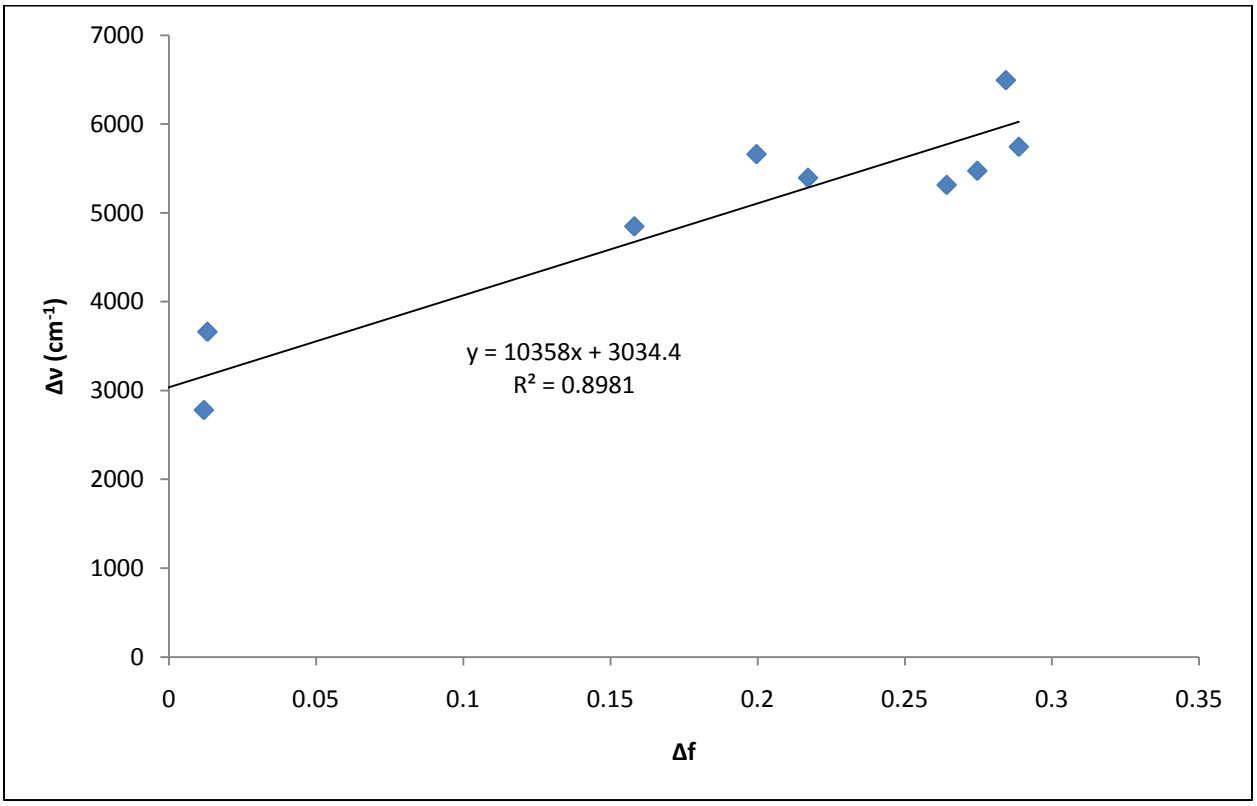

Figure 11: Lippert-Mataga plot of Stoke's shift ($\Delta\nu$) of **bydbc** against Δf in various solvents.

DFT B3LYP/6-31G(d) geometry optimization as well as TD-DFT spectral calculations were performed on **bydbc**. Molecular orbitals of this compound are shown in Figure 12. Calculations show that the $S_0 \rightarrow S_1$ transition occurs via an ICT (π, π^*) mechanism, and the $S_0 \rightarrow S_2$ transition is predicted to be (n, π^*). The electron density is distributed across the conjugated π system in the computed HOMO, with significant density on the dimethylaminobenzene moiety, while in the LUMO, electron density is centered around the carbonyl and benzofuran groups. Table 2 shows the molecular orbital calculations of **bydbc**, as well as the corresponding oscillator strengths (f) for each transition.

Table 2: Computed molecular orbital calculations of **bydbc**.

HOMO→LUMO	(CT, π, π*)
λ=445.6nm	f=1.065
HOMO-2→LUMO	(n, π*)
λ=424.6nm	f=0.0001

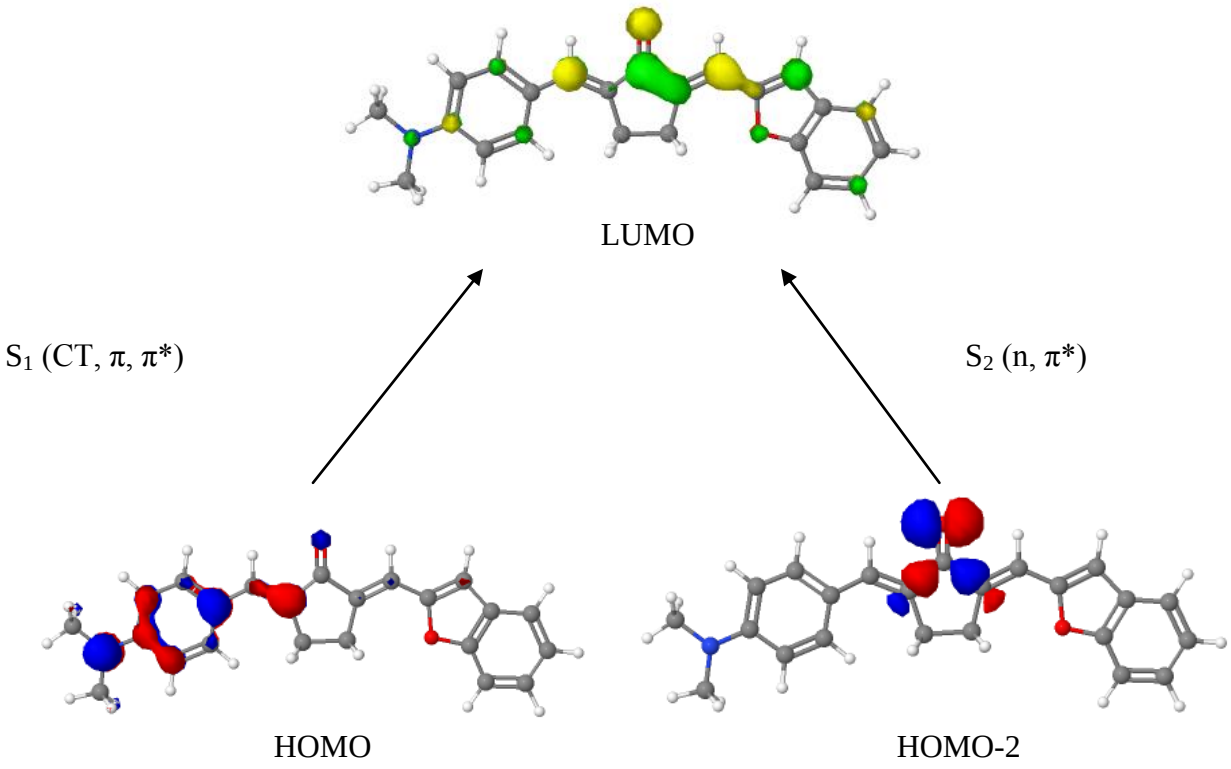

Figure 12: Computed molecular orbitals of **bydbc**.

Conclusions

Experimental data shows that **bydbc** exhibits solvatochromic properties in going from nonpolar to polar protic solvents. When plotted against Δf and $E_T(30)$, the spectroscopic characteristics show correlations with solvatochromism being more pronounced in the fluorescence spectral data; this is consistent with electronic transfer of charge. The fluorescence quantum yields and the fluorescence lifetimes show a strong solvent dependence, with quantum yields ranging from $4.9*10^{-3}$ (n-hexane) to 0.135 (dichloromethane) and lifetimes between 0.16 ns (acetone) to 1.1 ns (dichloromethane). The trend observed in the polar solvents is attributed to the energy gap law for internal conversion, which predicts an exponential dependence of k_{ic} on ΔE, the $S_0 \rightarrow S_1$ energy gap. Finally, quantum chemical calculations indicate that the $S_0 \rightarrow S_1$ transition occurs via an ICT (π, π^*) mechanism, with the $S_0 \rightarrow S_2$ transition predicted to be (n, π^*).

References

[1] Barnabus, M.V.; Liu, A.; Trifunac, A.D.; Krongauz, V.V.; Chang, C.T. *J. Phys. Chem.* **1992**, *96*, 212.

[2] Pivovarenko, V.G.; Klueva, A.V.; Doroshenko, A.O.; Demchenko, A.P. *Chem. Phys. Lett*. **2000**, *325*, 389.

[3] Das, P.K.; Pramanik, R.; Banerjee, D.; Bagchi, S. *Spectrochim. Acta. A*. **2000**, *56*, 2763.

[4] Doroshenko, A.O.; Grigorovich, A.V.; Posokhov, E.A.; Pivovarenko, V.G.; Demchenko, A.P. *Mol. Eng.* **1999**, *8*, 199.

[5] Kawamata, J.; Inoue, K.; Inabe, T. *Bull. Chem. Soc. Jpn*. **1998**, *71*, 2777.

[6] Connors, R.E.; Ucak-Astarlioglu, M.G. *J. Phys. Chem. A*. **2005**, *109*, 8275.

[7] Connors, R.E.; Ucak-Astarlioglu, M.G. *J. Phys. Chem. A.* **2003**, *107*, 7684.

[8] Suppan, P.; Ghonheim, N. *Solvatochromism*; Royal Society of Chemistry: Cambridge, 1997.

[9] Strauss, C.R.; Kreher, U.P.; Rosamilia, A.E.; Raston, C.L.; Scott, J.L. *Org. Lett.* **2003**, *5*, 3107.

[10] Strauss, C.R.; Rosamilia, A.E.; Giarrusso, M.A.; Scott, J.L. *Green Chem.* **2006**, *8*, 1042.

[11] Fery-Forgues, S.; Lavabre, D. *J. Chem. Ed*. **1999**. *76*, 1260.

[12] Lakowicz, J.R. *Principles of Fluorescence Spectroscopy*, 2nd ed.; Springer: New York, 2004.

[13] El-Sayed, M.A. *J. Chem. Phys*. **1963**, *38*, 2864.

[14] Klessinger, M.; Michl, J. Excited States and Photochemistry of Organic Molecules; VCH Publishers: New York, 1995.

[15] Lippert, E.Z. *Electrochem*. **1957**, *61*, 962.

[16] Mataga, N.; Kaifu, Y.; Koizum, M. *Bull. Chem. Soc. Jpn*. **1956**, *29*, 465.

Appendix A: Fluorescence Quantum Yield Sample Calculation

Connors

Quantum yield determination for **bydbc** in undegassed Acetone with red sensitive tube. Experiment 1

This QuickSheet demonstrates Mathcad's **cspline** and **interp** functions for connecting X-Y data.

Enter a matrix of X-Y data to be interpolated:

Enter spectral data for compound after converting to wavenumbers, multiplying intensity by lambda squared DO NOT normalize intensity. Insert data from Excel -right key, paste table.

data1 :=

21978.02	$2.13 \cdot 10^6$
21953.9	$2.14 \cdot 10^6$
21929.82	$2.09 \cdot 10^6$
21905.81	...

Click on the **Input Table** above until you see the handles, and enlarge it to see the matrix **data** used in this example.

data1 := csort(data1 ,0)

$X := data1^{\langle 0 \rangle}$ $Y := data1^{\langle 1 \rangle}$

Spline coefficients:

S1 := cspline(X ,Y)

Fitting function:

fit(x) := interp(S1 ,X ,Y ,x)

Sample interpolated values:

$fit(21000) = 2.382 \times 10^4$

$fit(18800) = 5.873 \times 10^4$

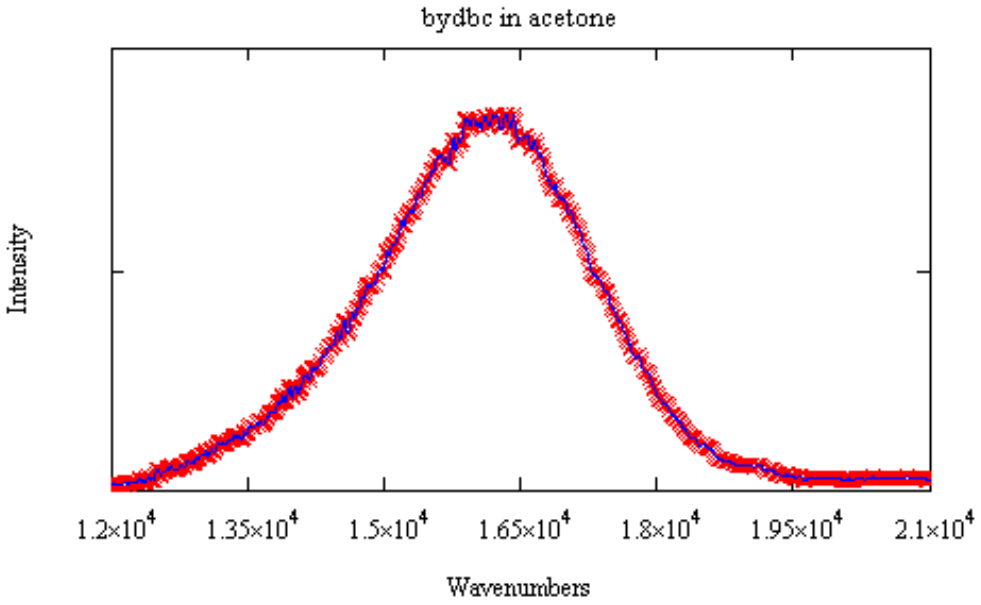

Correction factors for LS50B with red sensitive tube

DATA Limits 12,500-22,200 Wavenumbers

corrdata :=

	0	1
0	12500	4.43
1	12550	...

xdata := csort(corrdata,0)

A := corrdata$^{\langle 0 \rangle}$ B := corrdata$^{\langle 1 \rangle}$

Spline coefficients:

S := cspline(A,B)

Fitting function:

Fitting function:

corrfit(x) := interp(S,A,B,x)

corrspec(x) := corrfit(x)·fit(x)

$l := 12500, 12550 .. 22200$

$l =$

$1.25 \cdot 10^4$
$1.255 \cdot 10^4$
$1.26 \cdot 10^4$
...

corrspec(x)

fit(x)

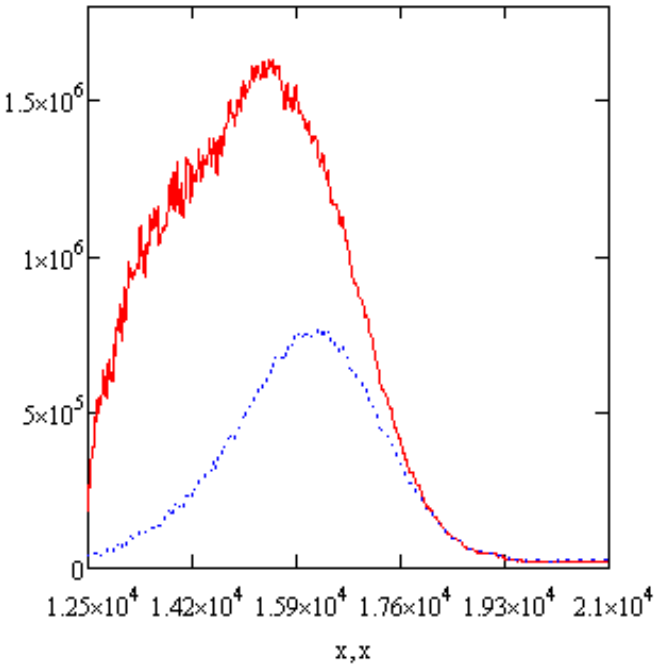

corrspec(l) =

$1.857 \cdot 10^5$
$3.188 \cdot 10^5$
$4.297 \cdot 10^5$
$5.206 \cdot 10^5$
...

$$\int_{12500}^{21000} \text{fit}(x)\,dx = 2.35 \times 10^9$$

$$\int_{12500}^{21000} \text{corrspec}(x)\,dx = 6.004 \times 10^9$$

Enter a matrix of X-Y data to be interpolated:

Enter spectral data for standard (fluorescein) after converting to wavenumbers, multiplying intensity by lambda squared DO NOT normalize intensities. Insert data from Excel -right key, paste table.

stdata :=

21978.02	$4.35 \cdot 10^6$
21953.9	$4.22 \cdot 10^6$
21929.82	...

Click on the **Input Table** above until you see the handles, and enlarge it to see the matrix **data** used in this example.

stdata := csort(stdata,0)

C := stdata$^{\langle 0 \rangle}$ D := stdata$^{\langle 1 \rangle}$

Spline coefficients:

S := cspline(C,D)

Fitting function:

sfit(x) := interp(S,C,D,x)

sfit(18000) = 6.496×10^{6}

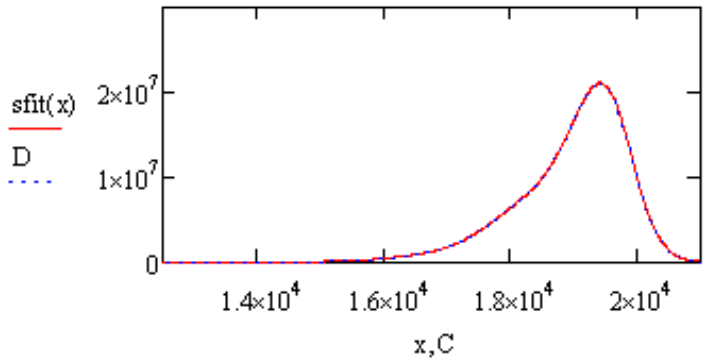

scorrspec(x) := corrfit(x)·(sfit(x))

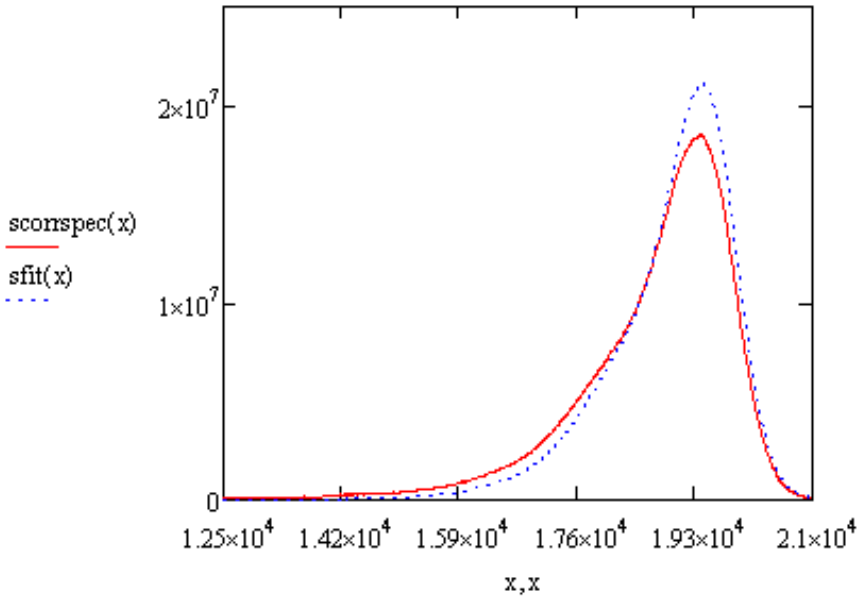

Compound

$$\int_{12500}^{21000} \text{corrspec}(x)\,dx = 6.004 \times 10^{9}$$

Standard

$$\int_{12500}^{21000} \text{scorrspec}(x)\,dx = 3.585 \times 10^{10}$$

Area under corrected compound curve

$$Dc := \int_{12500}^{21000} \text{corrspec}(x)\,dx$$

$$Dc = 6.004 \times 10^{9}$$

Area under corrected standard curve

$$Ds := \int_{12500}^{21000} \text{scorrspec}(x)\,dx$$

$$Ds = 3.585 \times 10^{10}$$

	Compound	Standard
Absorbance at l(ex)	Ac := 0.04971	As := 0.01143
Index of refraction	Acetone	NaOH
	nc := 1.359	ns := 1.413

quantum yield of standard

QYs := 0.95

$$QYc := QYs \cdot \left(\frac{As}{Ac}\right) \cdot \left(nc \cdot \frac{nc}{ns \cdot ns}\right) \cdot \left(\frac{Dc}{Ds}\right)$$

QYc = 0.034

Appendix B: Fluorescence Lifetime Sample Calculation

Analysis Function : Wed Apr 07 2010 at 10:34

****** one-to-four exponentials ******
***** Input Values *****

Decay curve : A1:462:597:dichloromethane_200chan
IRF curve : A1:462:462:dichloromethane_200chan

Start Time : 38.96
End Time : 50.11

Offset will be calculated
Shift will be calculated

Pre-exp. 1 : 1
Lifetime 1 : 1

***** Statistics *****
Job done after 6 iterations in 0.062 sec

Fitted curve : FLD Fit (4)
Residuals : FLD Residuals (4)

Autocorrelation : FLD Autocorrelation (4)
Deconvolved Fit : FLD Deconvoluted (4)

Chi2 : 2.298
Durbin Watson : 1.174
Z : -0.1363

Pre-exp. 1 : 1.613 ± 2.749e-002 (100 ± 1.705%)
Lifetime 1 : 1.108 ± 1.303e-002

F1 : 1
Tau-av1 : 1.108
Tau-av2 : 1.108

Offset : -22.75
Shift : 0.8711

****

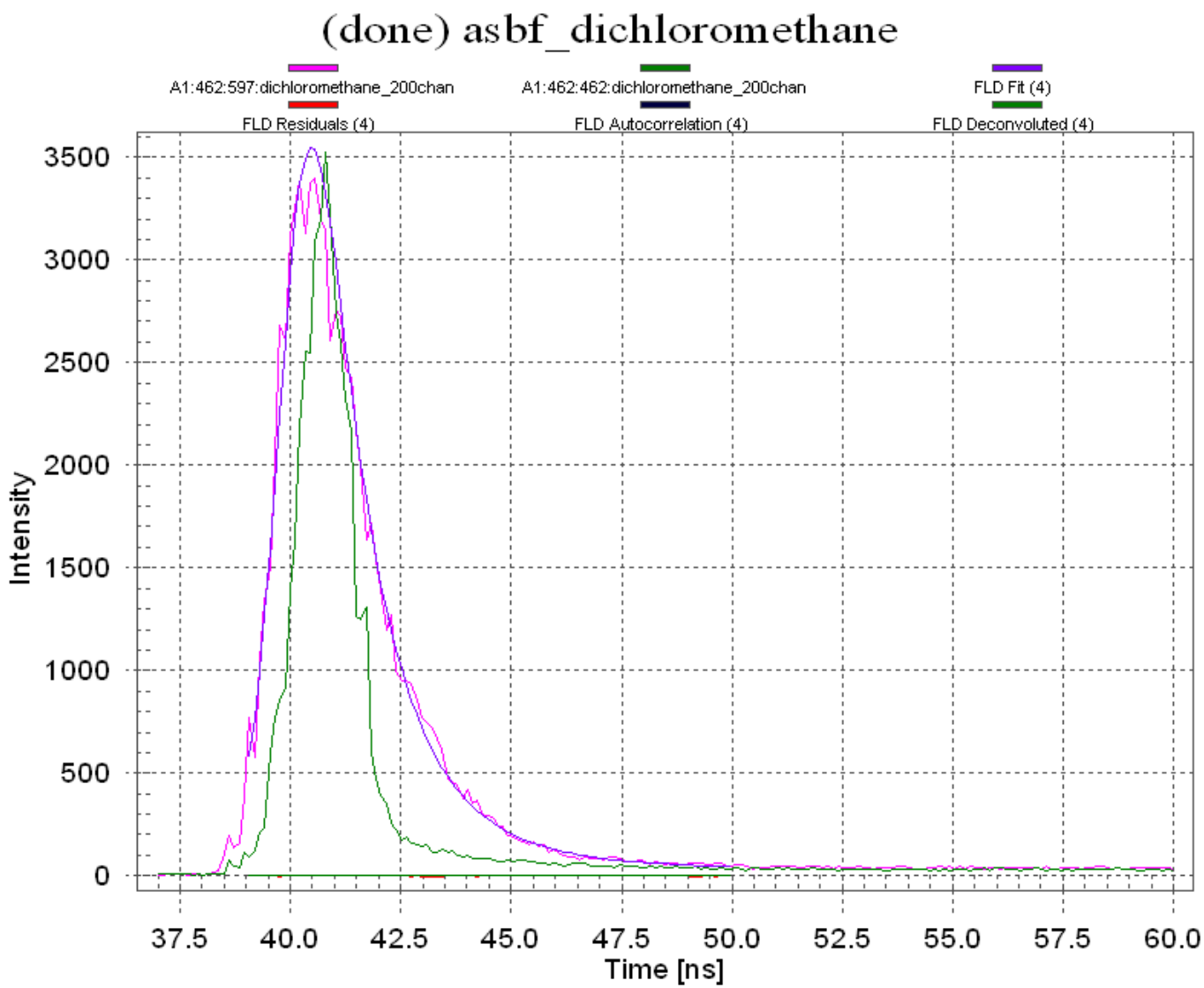
(done) asbf_dichloromethane
A1:462:597:dichloromethane_200chan
A1:462:462:dichloromethane_200chan
FLD Fit (4)
FLD Residuals (4)
FLD Autocorrelation (4)
FLD Deconvoluted (4)
Intensity
3500
3000
2500
2000
1500
1000
500
0
37.5
40.0
42.5
45.0
47.5
50.0
52.5
55.0
57.5
60.0
Time [ns]